A Plug-and-Play Spatially-Constrained Representation Enhancement Framework for Local-Life Recommendation

Hao Jiang Kuaishou Technology Beijing, China jianghao11@kuaishou.com

Yang Zeng Kuaishou Technology Beijing, China zhengchengyi@kuaishou.com Guoquan Wang Kuaishou Technology Beijing, China wangguoquan03@kuaishou.com

Wencong Zeng Kuaishou Technology Beijing, China zengwencong@kuaishou.com Sheng Yu Kuaishou Technology Beijing, China yusheng03@kuaishou.com

Guorui Zhou* Kuaishou Technology Beijing, China zhouguorui@kuaishou.com

Abstract

Local-life recommendation have witnessed rapid growth, providing users with convenient access to daily essentials. However, this domain faces two key challenges: (1) **spatial constraints**, driven by the requirements of the local-life scenario, where items are usually shown only to users within a limited geographic area, indirectly reducing their exposure probability; and (2) long-tail sparsity, where few popular items dominate user interactions, while many high-quality long-tail items are largely overlooked due to imbalanced interaction opportunities. Existing methods typically adopt a user-centric perspective, such as modeling spatial user preferences or enhancing long-tail representations with collaborative filtering signals. However, we argue that an item-centric perspective is more suitable for this domain, focusing on enhancing long-tail items representation that align with the spatially-constrained characteristics of local lifestyle services. To tackle this issue, we propose ReST, a Plug-And-Play Spatially-Constrained Representation Enhancement Framework for Long-Tail Local-Life Recommendation. Specifically, we first introduce a Meta ID Warm-up Network, which initializes fundamental ID representations by injecting their basic attribute-level semantic information. Subsequently, we propose a novel Spatially-Constrained ID Representation Enhancement Network (SIDENet) based on contrastive learning, which incorporates two efficient strategies: a spatially-constrained hard sampling strategy and a dynamic representation alignment strategy. This design adaptively identifies weak ID representations based on their attribute-level information during training. It additionally enhances them by capturing latent item relationships within the spatially-constrained characteristics of local lifestyle services, while preserving compatibility with popular items. Experiments on two real-world datasets and online A/B testing demonstrate that ReST

Permission to make digital or hard copies of all or part of this work for personal or classroom use is granted without fee provided that copies are not made or distributed for profit or commercial advantage and that copies bear this notice and the full citation on the first page. Copyrights for components of this work owned by others than the author(s) must be honored. Abstracting with credit is permitted. To copy otherwise, or republish, to post on servers or to redistribute to lists, requires prior specific permission and/or a fee. Request permissions from permissions@acm.org.

Conference'17, Washington, DC, USA

© 2025 Copyright held by the owner/author(s). Publication rights licensed to ACM. ACM ISBN 978-x-xxxx-xxxx-x/YYY/MM https://doi.org/10.1145/nnnnnnn.nnnnnn

significantly improves recommendation performance and exhibits strong plug-and-play flexibility in industrial applications.

CCS Concepts

• Information systems \rightarrow Recommender systems.

Keywords

Local-life Recommendation; Long-tail Recommendation; Spatial Constraints

ACM Reference Format:

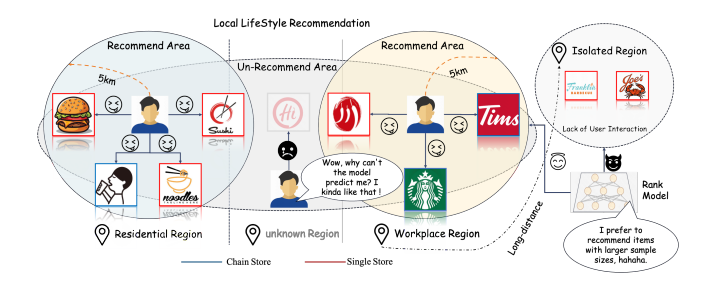


Figure 1: Illustration of local lifestyle recommendation: spatial constraints limit user-accessible candidates, leading to inaccurate predictions for disadvantaged items and causing the serious Matthew Effect.

1 Introduction

Online local lifestyle services utilize users' current geographic locations and historical behaviors to deliver context-aware recommendations for service-related content, such as short videos or nearby shops and restaurants [5, 41]. These services help people with everyday needs and have become increasingly popular in recent years [49, 50]. Major platforms like Kuaishou¹, Meituan², and Eleme³ have made such services, reaching tens of millions of users.

^{*}Corresponding author.

¹https://www.kuaishou.app.com

²https://www.meituan.com

³https://www.eleme.com

However, compared with traditional recommendation scenarios [18, 19], this domain poses unique challenges, primarily due to Imbalanced Exposure Across Category-Level Samples Under **Spatial Constraints**. Specifically, we divide the problem into two critical challenges in this domain. The first is the spatial constraints problem. As illustrated in Figure 1, items are typically only exposed to users within a limited geographic range, severely restricting their visibility and interaction opportunities. Due to spatial constraints, the pool of candidates is greatly reduced, making it difficult for longtail items to be exposed to a wider user. Furthermore, when users enter unfamiliar regions, the model may exhibit prediction bias against local items due to a lack of prior interactions [24, 25]. The second challenge is the long-tail problem. In the local lifestyle scenario, item exposure is uneven due to a large proportion of popular items, primarily chain stores (e.g., McDonald's, Starbucks), dominating the candidate pool. The Matthew effect [8] leads the system to favor these popular items, causing many small and medium-sized items, such as single stores, to suffer from insufficient exposure due to limited interaction data [6, 33, 34]. As a result, brand and category-level segmentation issues are more pronounced, making it difficult to accurately predict items from certain long-tail categories or brands. Moreover, as illustrated in the right part of Figure 1, users can rarely access items outside the areas they frequently visit, which worsens the long-tail problem and further impacts the user

Traditional methods typically rely on user modeling to capture user interests, leveraging deep neural networks such as GNNs, RNNs, and self-attention mechanisms [10-13, 42]. However, these approaches struggle to overcome spatial constraints and thus exhibit suboptimal performance when directly applied to local lifestyle scenarios [14]. To address this issue, recent work has incorporated spatiotemporal information into user modeling. This has been achieved either by constructing user behavior features through search-based strategies or by designing novel architectures that softly inject spatial and temporal signals, such as StEN [5], BASM [25], and STKG [41]. Despite these advances, most existing methods remain user-centric and fail to effectively adapt to the dynamic and regionally diverse nature of local lifestyle services. Moreover, they are not well-suited to scenarios with sparse user interactions. Furthermore, when user interaction data are sparse, recommendation performance deteriorates significantly, causing long-tail items to suffer from limited exposure and poor prediction accuracy. While prior works have made progress in long-tail recommendation by improving ID representations for infrequent items [29, 30, 32], it often neglects the latent relationships among items constrained by spatial factors. Therefore, they struggle to capture the dynamic nature of spatially-constrained local lifestyle recommendations.

To address the limitations of existing methods, this paper proposes ReST, a Plug-and-Play Representation Enhancement Framework for Spatially-Constrained Long-Tail Item Recommendation in local lifestyle Services. Our framework specifically targets the challenges of spatial constraints and long-tail problems while also accounting for the dynamic nature of candidate items in this domain. Specifically, ReST consists of two key modules: (1) a Meta ID Warm-Up Network, and (2) a Spatially-Constrained ID Representation Enhancement Network (SIDENet). First, we

leverage attribute-level semantic information to initialize a fundamental ID representation, which is enhanced through weighted attribute selection and semantic information injection. This module ensures model convergence during training, which is particularly beneficial for long-tail items. Second, in SIDENet, we propose a novel spatially-constrained hard sampling strategy. Our approach aims to uncover latent relationships among items confined to spatially-constrained regions, rather than relying purely on user interactions in traditional methods. Furthermore, to accommodate to the dynamic nature of candidate items in local lifestyle services, we design a dynamic representation alignment strategy. This mechanism instantly adjusts the enhancement weights based on the current quality of ID representations with their attribute-level information during model training. It effectively balances collaborative and semantic signals, enhancing the representation of long-tail items while maintaining robustness for popular items. Notably, ReST is a Plug-and-Play framework that can be seamlessly integrated into any existing recommendation model, demonstrating strong generalization with various backbone architectures.

We conduct comprehensive experiments on two real-world local lifestyle recommendation datasets. Compared with existing spatially-constrained and long-tail recommendation methods, our method achieves substantial performance gains. Further ablation studies validate the effectiveness of each module and demonstrate the overall robustness of our approach. Notably, our model also achieves significant improvements on cold-start datasets, demonstrating its strong generalization capability for long-tail items and sparse interaction scenarios. In addition, we perform online A/B testing within real-world applications at the Kuaishou platform. The results show that our model significantly outperforms strong base model in terms of gross merchandise value (GMV) and order volume, particularly for long-tail items.

In summary, our major contributions are as follows.

- We design a novel plug-and-play representation enhancement module that includes a meta ID warm-up network and a spatiallyconstrained ID representation enhancement network.
- We propose an item-centric method tailored to the characteristics of local lifestyle services, enhancing the performance and robustness of recommendation models for long-tail items under sparse supervised signals.
- We conduct offline experiments to demonstrate the effectiveness of ReST. In addition, online A/B testing shows that ReST increases online GMV by 2.804% and the number of orders by 1.285%.

2 Related work

2.1 Spatially-Constrained Recommendation

Spatially-constrained recommendation aims to provide personalized recommendations while considering users' spatial constraints and mobility patterns. Early methods primarily relied on simple distance-based filtering or basic geographic features [51, 52]. With the development of deep learning, more sophisticated approaches have emerged to model spatiotemporal user preferences. ST-PIL [21] introduces a geohash-based filtering mechanism to process user behavior sequences, enabling more focused modeling of user interests within specific geographic regions. Building upon this, TRISAN [22] advances the field by modeling not only physical

distances but also semantic similarities between locations through attention mechanisms. SPCS [23] further enhances spatial modeling by explicitly incorporating user-merchant distance relationships through a spatiotemporal graph transformer architecture. More recent approaches have explored integrated solutions. OFRS [24] proposes a weighted fusion of spatiotemporal and ID features, while BASM [25] introduces multi-layered spatial-aware semantic modeling. CLSPRec [26] leverages trajectory encoding and contrastive learning to capture user preferences across different distance ranges. However, in local lifestyle recommendations, while spatial constraints significantly influence user behavior, the traffic is dominated by a small portion of items. This creates a unique challenge where spatial constraints and long-tail issues are inherently intertwined, requiring a solution to address both aspects simultaneously. Therefore, we propose a spatially-constrained ID representation enhance network that jointly addresses these limitations.

2.2 Long-Tail Item Recommendation

Long-tail item recommendation focuses on improving the exposure and recommendation accuracy for less popular items while maintaining overall system performance. Early approaches like DropoutNet [29] simulated cold-start scenarios by randomly dropping interaction information during training. Pan et al. [30] introduced meta-learning to generate embeddings for new items based on previously learned patterns. The field has evolved with more sophisticated approaches. CMDP [31] formulates the problem as a constrained Markov decision process to ensure fair exposure across popularity levels. CL4SRec [32] leverages contrastive learning to extract self-supervised signals from user behavior sequences. Recent works like LOT-CRS [33] and HIM [34] have focused on enhancing long-tail item understanding through pre-training tasks and hierarchical interest modeling. Latest developments include UIH [35], which prioritizes long-tail items during user history sampling, and EDGE [38], which optimizes embedding norms and directions to better reflect item popularity. However, existing methods primarily focus on general long-tail item modeling without considering the unique characteristics of local lifestyle services, where accelerating the exposure of high-potential long-tail videos under spatial constraints is crucial for business success. To address this specific challenge, we propose a meta ID warm-up network that effectively enhances representations for spatially constrained long-tail items while maintaining quality of popular items representation.

3 Preliminaries

3.1 Problem Definition

Local lifestyle recommendation systems are designed to serve users' daily needs, such as food, beverages, and entertainment. The core objective is to predict a user's next payment behavior based on their historical actions, from candidate items located within a fixed spatial radius, such as 5 kilometers. In real-world applications, a distance-based filter is often applied prior to the model scoring step, pre-selecting qualified candidate items. Given a user set (\mathcal{U}) , an item set (\mathcal{V}) , and the subset of items within the spatial radius range (\mathcal{V}^D) , where D denotes the pre-defined distance limit, we can construct sequences from user historical behavior as $B = (v_1, v_2, \ldots, v_{|\mathcal{H}|})$, where $v_i \in \mathcal{V}$ is the user historical items and $|\mathcal{H}|$ is the length

of user historical sequence. The recommendation model first recalls items within the spatial range $(V_u^D \subseteq V^D)$. Then, our main task is to predict the recommendation scores for the candidate items. Based on these scores, we then recommend a list of k items, $\{v_{i+1}, v_{i+2}, \ldots, v_{i+k}\}$, to a given user u at a specific location.

3.2 Basic Recommend Tower

As shown in the left part of Figure 2(a), we employ a attention-based user interest layer [49] with candidate items feature and integrate the characteristics of local-life scenarios to predict ranking score.

3.2.1 Embedding Layer. In this part, we use an embedding layer to encode model features. Specifically, we select the user ID (ID_u) and their historical behavior sequence, denoted as $B = (v_1, v_2, \ldots, v_{|H|})$, as the user-side features. For item-side features, we select the item ID (ID_i), along with basic attribute information such as brand (B) and category (C) and location (GeoHash). These categorical features are then transformed into high-dimensional binary vectors as model inputs, where $\mathbf{E}_u \in \mathbb{R}^d$, $\mathbf{E}_i \in \mathbb{R}^d$, $\mathbf{X} = (\mathbf{v}_1, \mathbf{v}_2, \ldots, \mathbf{v}_{|H|}) \in \mathbb{R}^{n \times d}$, $\mathbf{E}_B \in \mathbb{R}^d$, and $\mathbf{E}_C \in \mathbb{R}^d$ represent the embeddings of user ID, item ID, user behaviors, item brand, and item category, respectively.

3.2.2 User Interest Layer. Following the structure of FIM [49], we perform weighted-sum pooling on a candidate item and the user's historical behavior sequence to adaptively select relevant behaviors and capture the user-interest vector as shown in Eq. (1).

$$\mathbf{V}_{u} = \sum_{j=1}^{|\mathbf{H}|} a\left(\mathbf{v}_{j}, \mathbf{v}_{t}\right) \mathbf{v}_{j} = \sum_{j=1}^{|\mathbf{H}|} w_{j} \mathbf{v}_{j}, \tag{1}$$

where $\mathbf{v}_j \in \mathbb{R}^d$ denotes the embedding of the j-th historical behavior, \mathbf{v}_t is the embedding of the target item, $a(\cdot)$ is a feed-forward attention network that outputs the activation weight w_j , and $\mathbf{V}_u \in \mathbb{R}^d$ represents the final user interest vector.

3.2.3 Prediction Layer. Given the user interest vector, along with the item ID and attribute embeddings, we adopt a multi-layer fully connected network as the main task tower to predict the probability P_{ui} of user interaction, as shown in Eq. (2).

$$\mathbf{P}_{ui} = \mathbf{Sigmoid} \left(\mathcal{MLP}(\mathbf{V}_u \parallel \mathbf{E}_u \parallel \mathbf{E}_i \parallel \mathbf{E}_B \parallel \mathbf{E}_c) \right), \tag{2}$$

where "||" denotes concatenation product, and **Sigmoid** is the activation function. In our ReST, \mathbf{E}_{i}^{warm} (enhanced ID representation) is used to replace \mathbf{E}_{i} .

4 METHODOLOGY

4.1 Model Structure

In this section, we introduce the structure of our proposed model, as illustrated in Figure 2(a). Specifically, the model is divided into two main components: the basic recommendation tower, shown on the left side of Figure 2(a), and our novel Spatially-Constrained ID Enhancement Network (SIDENet), depicted on the right of Figure 2(a). The basic recommendation tower is interchangeable (as discussed in Section 3.2), which enhances the practicality and ease of implementation of our method. We further evaluate its variants in Section 5.3. Within SIDENet, we propose two distinct parts: the Meta ID Warmup Network, which aims to initialize item representations with their

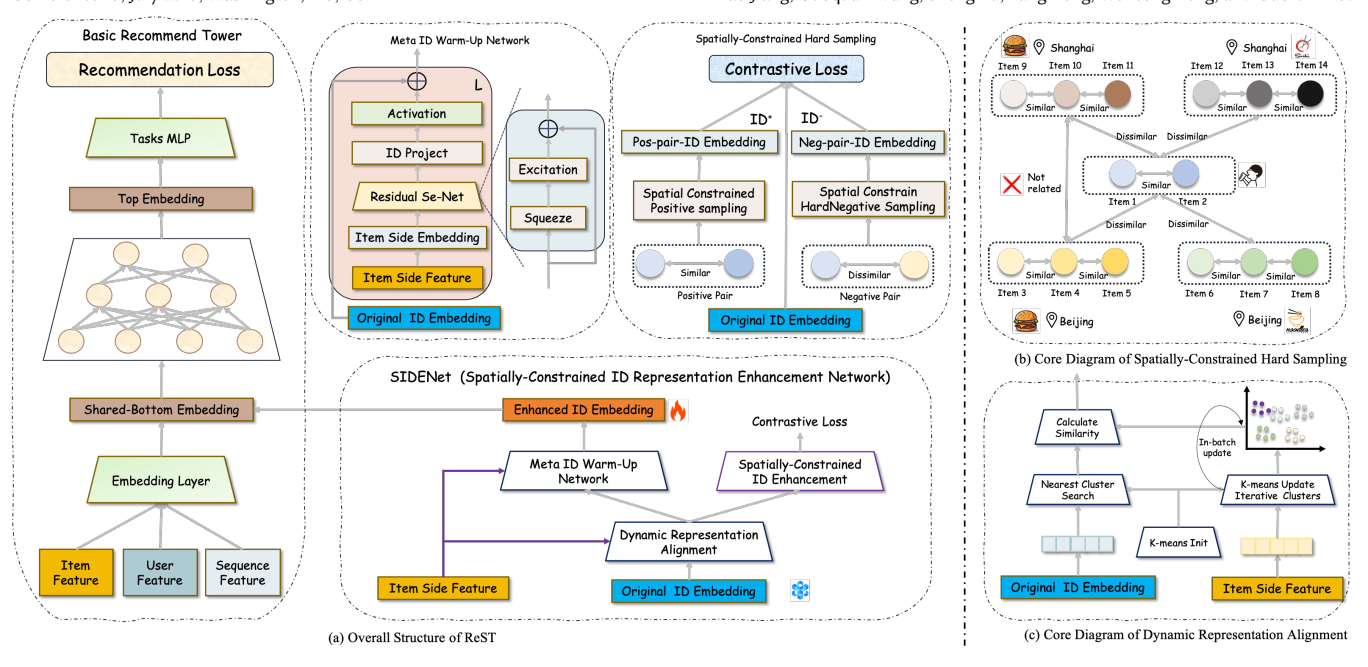


Figure 2: This figure illustrates the overall structure and key components of the ReST model. Specifically:(a) shows the architecture of ReST, where the Basic Recommendation Tower can be any recommendation model. In this paper, we adopt DIN as the ranking backbone. (b) depicts the core concept of spatially-constrained sampling, where prior knowledge is leveraged to retrieve semantically similar items, and a spatially-constrained hard sampling strategy is applied. For instance, "Burger Restaurants" located in Beijing and Shanghai should not be considered similar due to differences in their target user location and competing item environments. (c) presents the dynamic representation alignment strategy, which adaptively determines the enhancement strength for different ID representations.

basic attribute information, and the Spatially-Constrained ID Enhancement Network, which includes a spatially-constrained hard negative sampling strategy and a dynamic representation alignment strategy. This network dynamically improves the quality of ID representations by considering characteristics of local lifestyle scenarios, especially for long-tail items.

4.2 Meta ID Warm-up Network

This module serves as the foundation of SIDENet, enhancing ID representations using attribute information. It consists of two key components: meta feature selection and meta feature injection.

4.2.1 Meta Feature Selection. Considering that basic item attribute features converge significantly more effectively than ID-based features, a natural approach is to leverage these attributes to assist ID representation learning. Specifically, we adopt a squeeze-and-excitation network (SeNet) [20] to adaptively reweight the importance of item attribute features such as brand and category, which play a crucial role in local lifestyle recommendation.

$$F_i = SeNet(E_b, E_c), \tag{3}$$

where F_i , E_b , and E_c are representations of the item attribute feature, original item ID, item brand, and item category, respectively.

4.2.2 Meta Feature Injection. After obtaining the weighted attribute-level ID representation, this module injects them into the same dimensional space as the ID embeddings by using a multi-layer

perceptron (MLP) with residual connections, as shown in Eq. (4).

$$\mathbf{E}_{i}^{warm} = \mathcal{MLP}(\mathbf{F}_{i}) + \mathbf{E}_{i}, \tag{4}$$

where "+" operator indicates the residual connection, \mathbf{E}_i is the original ID representation, and $\mathbf{E}_i^{warm} \in \mathbb{R}^d$ is the warm-up ID representation that carry attribute-level semantic information.

4.3 Spatially-Constrained ID Enhancement

Relying solely on intrinsic attribute information has certain limitations. On one hand, highly similar items may result in indistinguishable ID representations. On the other hand, this warm-up approach can be overly rigid, depends partially on supervised signals, and therefore may not achieve optimal performance.

4.3.1 Spatially-Constrained Hard Sampling Strategy. Employing a self-supervised contrastive learning method is more appropriate, which is illustrated in Figure 2(b). However, conventional methods that construct positive and negative pairs based on "co-occurrence" relationships, such as user-to-item (U2I) [46] and item-to-item (I2I) [47] approaches, prove ineffective in local lifestyle scenarios for two key reasons. First, co-occurrence signals are heavily biased toward a few dominant items, while long-tail items suffer from extreme sparsity. Second, items sharing the same brand and category within close location often exhibit similar spatial characteristics and user interaction patterns. Therefore, we propose a tunnel-based hard negative sampling strategy comprising three stages: (1) prior-knowledge-based hard sampling, (2) similarity-aware hard sampling, and (3)

Algorithm 1 Dynamic Representation Alignment Strategy

Input: Item brand **B**, item category **C**, item ID embedding \mathbf{E}_i , number of clusters |N|

Output: Adaptive enhancement weight α_i for each item

- 1: Initialize K-means with |N| clusters
- 2: Initialize parameters of $\mathcal{MLP}(\cdot)$ of Eq. (7)
- 3: **for** j = 1 to *MaxIterations* **do**
- 4: $A \leftarrow \mathcal{MLP}(B, C)$ > Project to semantic space
- 5: $R \leftarrow K$ -means.Update(F) \triangleright Update cluster centroids
- 6: $\mathbf{M} \leftarrow \text{K-means.IndexSearch}(\mathbf{E}_i, \mathbf{R}) \triangleright \text{Find nearest centroid}$
- 7: Compute α_i using Eq. (10) \triangleright Enhancement weight
- 8: end for
- 9: **return** α_i

spatially-constrained hard sampling, which progressively filters more suitable positive and negative samples.

- (1) Prior-Knowledge Hard Sampling. By leveraging the natural similarity between items with the same attributes, this sampling strategy improves the model's sensitivity to scenario-specific attribute signals. Specifically, positive and negative pairs are sampled within each training batch based on item brand and category. To maintain a balance between positive and negative samples and ensure sufficient diversity during training, the sampling number (K) is dynamically adjusted according to the underlying data distribution.
- (2) Similarity-Aware Hard Sampling. Numerous candidate samples may be produced after prior-knowledge hard sampling, making an effective selection of hard negatives essential. We introduce a similarity-aware hard sampling strategy. Given a target item embedding $E \in \mathbb{R}^d$, we construct a candidate matrix $E_s \in \mathbb{R}^{n \times d}$ using items from the same training batch that do not share the same category or brand as the target item. We then compute embedding similarity scores and select the most informative negatives based on these scores, as shown in Eq. (5).

$$s_i = sim(E, E_s^i), \quad i = 1, 2, ..., o$$
 (5)

where o is the batch size. Finally, the model selects Top-K similar negative items as hard negatives.

(3) Spatially-Constrained Negative Sampling. Considering that items within a fixed spatial radius often share similar spatial characteristics and user interaction patterns, we calculate the distances among each candidate sampling items, as shown in Eq. (6).

$$d_{ij} = \text{Haversine}_d(\text{GeoHash}_i, \text{GeoHash}_i),$$
 (6)

where $GeoHash_i$ denotes the location code of item i [54], and $Haversine(\cdot)$ represents the function calculating the haversine distance [48]. Finally, the model selects items within a predefined Haversine distance threshold as hard negatives, while also applying the same constraint to identify high-quality positive samples.

- **(4) Final Pairs Construction.** Positive and negative pairs for the spatially-constrained problem are constructed as follows:
- <Trigger Item, Pos Item>: Item pairs that share the same category or brand, selected through steps (1) (2) and (3).
- < Trigger Item, Neg Item>: Hard negative K items that not share category or brand, selected through steps (1) (2) and (3).
- 4.3.2 Dynamic Representation Alignment Strategy. To balance collaborative signals with attribute-level semantic information, we

propose a dynamic representation alignment strategy, illustrated in Figure 2(c). This strategy first generates semantic clusters by K-means algorithm [55] and then adaptively evaluates the quality of each representation based on well-trained attribute-level semantic embedding, dynamically adjusting the enhancement strength. By partially aligning the ID representations with their corresponding semantic cluster projections, the model not only stabilizes the training process but also produces more robust item embeddings. Specifically, we first project item attribute feature into a semantic cluster representation space, as detailed in Eq. (7).

$$\mathbf{A} = \mathcal{MLP}(\mathbf{E}_B||\mathbf{E}_c),\tag{7}$$

Then, we feed $A \in \mathbb{R}^d$ into the K-means algorithm, which iteratively refines the cluster centroids through optimization.

$$\mathbf{R} = \mathbf{K}\text{-}\mathbf{means}(\mathbf{A}, N), \tag{8}$$

where $\mathbf{R} \in \mathbb{R}^{|N| \times d}$ denotes the centroid representations of the K-means clusters, with |N| representing the total number of clusters. We then identify the nearest cluster centroid using Eq. (9).

$$M = NearestRep(E_i, R), \tag{9}$$

where M is the nearest centroid index of K-means cluster. Finally, we calculate the weight with M-th centroid, as shown in Eq. (10).

$$\alpha_i = 1 - \frac{1}{2} \left(\frac{\mathbf{E}_i^{\mathsf{T}} \mathbf{R}_{\mathsf{M}}}{\|\mathbf{E}_i\| \cdot \|\mathbf{R}_{\mathsf{M}}\| + \varepsilon} + 1 \right), \tag{10}$$

where α_i denotes the enhancement weight for item i, " $|\cdot|$ " denotes the ℓ _2 norm, ε is a constant for numerical stability, the similarity is normalized into the [0,1] range, and R_M is the representation of M-th centroid. Then, we modify Eq. (11) by introducing it as a weight into the spatiotemporal contrastive loss to adaptively emphasize hard samples. The overall algorithm is shown in Algorithm 1.

$$\mathbf{E}_{i}^{warm} = \alpha_{i} \times \mathcal{MLP}(\mathbf{S}_{i}) + \mathbf{E}_{i}. \tag{11}$$

4.4 Model Training

During the model training phase, we adopt the *Cross-Entropy* loss [53] as the primary optimization objective for recommendation, as shown in Eq. (12).

Loss =
$$-\frac{1}{|S|} \sum_{(x,y) \in S} (y \log P(x) + (1-y) \log(1 - P(x))),$$
 (12)

where S denotes the training set, |S| is its total size, x represents an input sample, and $y \in [0,1]$ is the ground-truth label. The output P(x) denotes the predicted probability of x being purchased, obtained from the network's sigmoid activation layer with Eq. (2). Subsequently, we construct a contrastive learning loss, using InfoNCE loss [1], based on the spatially-constrained hard sampling strategy and the dynamic representation alignment strategy. This loss is incorporated as an auxiliary task alongside the primary recommended objective, as shown in Eq. (13).

$$\operatorname{Loss}_{cl} = -\sum_{i \in |O|} \log \left(\frac{\frac{\exp(\mathbf{E}_{i}, \mathbf{E}_{i*})}{\tau}}{\sum_{i \in |K|} \frac{\exp(\mathbf{E}_{i}, \mathbf{E}_{j})}{\tau}} \right), \tag{13}$$

where O denotes the set of all items, K is the number of negative samples, and "·" represents the dot product similarity. Formally, this module integrates the contrastive learning loss into the overall

training objective, enabling end-to-end optimization of the recommendation model. The final loss is defined in Eq. (14).

$$Loss_{final} = Loss + \alpha_1 * \alpha_2 * Loss_{cl}, \tag{14}$$

where α_1 is the enhancement weight introduced in Eq. (10), and α_2 is a hyperparameter balancing the unified recommendation loss.

5 Experiment

To thoroughly evaluate our approach, we design a series of experiments to answer the following research questions:

- **RQ 1**: How does our method compare with state-of-the-art baselines in terms of both effectiveness and computational efficiency?
- RQ 2: Can our method maintain its effectiveness when integrated into various recommendation frameworks?
- RQ 3: How does each component impact the performance of the overall framework?
- RQ 4: How do hyper-parameters influence the performance of the overall framework?
- RQ 5: How does ReST perform in real-world online recommendation scenarios according to practical metrics?

5.1 Experimental Settings

- 5.1.1 Datasets. We conduct extensive experiments on both public and production datasets to evaluate the effectiveness of our proposed ReST framework against state-of-the-art baselines.
- Public Dataset. We use the Eleme dataset [41], a large-scale benchmark comprising takeaway recommendation data. It includes users' purchase histories along with rich contextual features such as spatial and temporal information.
- Production Dataset. The Kuaishou dataset is a real-world dataset sampled from one year of transaction logs (March 2024 to March 2025) on Kuaishou's local lifestyle platform. We sample user transaction behaviors (pay order) and use them as prediction targets to supervise recommendation training.

Table 1: Comparison of Datasets.

Datasets	Sample	User	Item	Avg. action length
Eleme	1,440,600	70,389	2,092,944	41.008
Kuaishou	1,046,100	72,805	81,487	8.895

5.1.2 Baselines. To evaluate the effectiveness of our model, we compare it with the following representative baselines: Representation Learning Methods: DIN [39], RCL [40]. These methods focus on learning effective representations from user-item interactions. Specifically, they employ various techniques to capture user preferences and item characteristics in a low-dimensional embedding space, where the semantic relationships between users and items can be better modeled. Spatially-Constrained Methods: TRISAN [22], OFRS [24], BASM [25]. These approaches explicitly model the complex relationships between time and location factors, considering how user preferences vary across different times and locations to make more contextually relevant recommendations.

5.1.3 Parameter Settings. In our experimental setup, we maintain consistent configurations across all methods to ensure fair comparisons. The batch size is uniformly set to 10,240, and the optimal

settings are selected based on model performance on the validation data. For both the Eleme and Kuaishou datasets, we set the embedding dimension for each categorical feature to 8, with the predict MLP tower dimensions configured as [32, 16, 1]. We employ AdamW as the optimizer, applying learning rates of 0.1 and 0.2 for Kuaishou and Eleme respectively, with a steplr scheduler that decays the learning rate by a factor of 0.9 every 500 steps. For the contrastive learning hyperparameters, we configure the positive sample constraint range to 30km and the negative sample constraint range to 10km, utilizing 9 hard negative samples in the training process. The contrastive learning loss weight is set to 0.01, and we implement 50 clustering centers. All experiments are conducted on two GPUs, each equipped with 48GB of memory.

5.1.4 Experimental Metircs. To comprehensively evaluate the performance of our recommendation model, we employ three widely adopted metrics: AUC (Area Under the ROC Curve) [43], MRR (Mean Reciprocal Rank) [44], and NDCG@k (Normalized Discounted Cumulative Gain) with k set to 5 and 10 [45]. AUC measures the model's ability to distinguish between positive and negative samples, providing a holistic view of the recommendation system's discriminative power. MRR evaluates the average position of the first relevant item in the recommendation list, reflecting the model's capability to place the correct recommendation at higher ranks. NDCG@k is a position-aware metric that assigns higher weights to recommendations ranked at higher positions, with k set to 5 and 10 to assess both immediate and slightly longer recommendation lists.

5.2 Overall Performance (RQ 1)

Table 2 presents the overall performance comparison between ReST and various baseline methods on two real-world datasets (Kuaishou and Eleme [41]). Because public datasets have limited attribute information compared to real-world systems, we align our model features with the baselines to verify our design's effectiveness.

Performance in Full Dataset. From the experimental results, we have the following key observations: First, ReST consistently achieves superior performance across most metrics on both datasets. Specifically, on the Kuaishou dataset, ReST outperforms the best baseline RCL [40] by 3.58% in terms of AUC and improves NDCG@10 by 1.05%. This demonstrates the effectiveness of our proposed framework in handling local lifestyle service scenario. Second, while spatiotemporal methods (TRISAN [22], OFRS [24], BASM [25]) show competitive performance by considering spatial information in user modeling, they fail to effectively address the long-tail issue. For instance, BASM [25] achieves strong results on Eleme dataset but falls short on Kuaishou dataset, likely due to its insufficient enforcement of spatial constraints in the recommendation procThird, representation learning methods like DIN [39] and RCL show limitations when dealing with spatially-constrained problem. Although RCL performs well in certain metrics, its performance is inconsistent across datasets, suggesting that purely focusing on representation enhancement without considering spatial information is insufficient for local lifestyle scenario. ReST's superior performance stems from jointly addressing spatial constraints and long-tail sparsity via the meta ID warm-up and spatially constrained ID enhancement networks, enabling better handling of both popular chains store and underrepresented local store.

Methods	Kuaishou			Eleme				
Methous	AUC	MRR	NDCG@5	NDCG@10	AUC	MRR	NDCG@5	NDCG@10
DIN (KDD 18) [39]	0.6946	0.3977	0.3911	0.4595	0.5653	0.1911	0.1615	0.2422
TRISAN (CIKM 21) [22]	0.7039	0.3968	0.3978	0.4633	0.5283	0.2015	0.1753	0.2545
OFRS (CIKM 23) [24]	0.7216	0.4074	0.4101	0.4784	0.5220	0.1920	0.1634	0.2455
BASM (ICDE 23) [25]	0.7193	0.4168	0.4187	0.4796	0.5752	0.2318	0.2115	0.2945
RCL (CIKM 24) [40]	0.7078	0.4327	0.4332	0.4891	0.5730	0.1542	0.1413	0.2164
ReST (Ours)	0.7436	0.4266	0.4345	0.4996	0.5830	0.2194	0.1973	0.2882

Table 2: Overall performance comparison. The best results are in boldface and the second-best results are underlined.

Table 3: Overall performance comparison on the cold-start dataset where items appear fewer than three times.

Methods	Kuaishou-cold-start				Eleme-cold-start			
Methods	AUC	MRR	NDCG@5	NDCG@10	AUC	MRR	NDCG@5	NDCG@10
DIN (KDD 18) [39]	0.6720	0.3846	0.3775	0.4429	0.5597	0.2184	0.1967	0.2797
TRISAN (CIKM 21) [22]	0.6741	0.3790	0.3779	0.4377	0.5237	0.1997	0.1711	0.2510
OFRS (CIKM 23) [24]	0.5409	0.2038	0.1797	0.2608	0.5067	0.1836	0.1526	0.2326
BASM (ICDE 23) [25]	0.6623	0.3974	0.3953	0.4442	0.5714	0.2263	0.2049	0.2890
RCL (CIKM 24) [40]	0.6397	0.3186	0.2942	0.2946	0.5736	0.1523	0.1399	0.2154
ReST (Ours)	0.6866	0.3871	0.3954	0.4481	0.5824	0.2223	0.2018	0.2901

Performance in Cold-start Dataset. When evaluating the challenging cold-start scenarios where items appear fewer than three times, we observe a natural performance in Table 3 degradation across all methods. However, ReST maintains its superiority by achieving the best results on both datasets, with AUC reaching 0.6866 on Kuaishou and 0.5824 on Eleme, demonstrating its robust generalization ability. Notably, while other methods like OFRS show significant performance drops with AUC decreasing from 0.7216 to 0.5409 on Kuaishou, ReST exhibits more stable performance thanks to its meta ID warm-up network, which effectively learns to generate initial embeddings for cold-start items. This is particularly evident in the Eleme dataset, where ReST outperforms the second-best method BASM by achieving a better AUC of 0.5824 versus 0.5714 and comparable NDCG@10 of 0.2901 versus 0.2890, indicating its strong capability in handling cold-start recommendations.

Computational Efficiency Comparison. Table 4 summarizes the model-scale and online-inference overhead comparison across various recommendation methods when ReST is applied. Our method has 0.79M parameters on Kuaishou and 142.15M parameters on Eleme, comparable to mainstream methods such as DIN, TRISAN, and RCL, and only slightly lower than BASM. Furthermore, ReST's inference time on both datasets is significantly lower than other methods. This demonstrates that ReST handles spatial constraints and long-tail problems without introducing redundant parameters, maintaining efficient model design.

5.3 Generalization Ability Analysis (RQ 2)

As illustrated in Table 5, integrating ReST into various recommendation models demonstrates significant performance improvements. For the DIN model, ReST achieves notable improvements with AUC increasing by 1.62%, MRR by 2.12%, NDCG@5 by 4.55%, and NDCG@10 by 3.98%. These improvements can be attributed to ReST's meta ID warm-up network, which effectively enhances the representation quality of merchant IDs, particularly beneficial for

Table 4: Parameter and inference time comparison by applying ReST to various recommendation learning methods.

Method	Paran	n. (M)	Time (ms/batch)		
	Kuaishou	Eleme	Kuaishou	Eleme	
DIN	0.79 M	142.15 M	297.74 ms/b	306.56 ms/b	
TRISAN	0.79 M	142.15 M	485.06 ms/b	482.77 ms/b	
OFRS	0.80 M	142.16 M	1668.01 ms/b	1667.33 ms/b	
BASM	0.8 5M	142.21 M	446.08 ms/b	452.38 ms/b	
RCL	0.79 M	142.15 M	2294.82 ms/b	2276.49 ms/b	
ReST	0.79 M	142.15 M	303.55 ms/b	303.10 ms/b	

attention-based mechanisms in DIN. The most substantial gains are observed with the TRISAN [22] model, where AUC improves by 5.90%, MRR by 11.54%, NDCG@5 by 12.57%, and NDCG@10 by 10.62%. This remarkable enhancement stems from ReST's spatially-constrained ID enhancement network, which effectively captures spatial constraints while addressing long-tail sparsity issues, particularly complementing TRISAN's sequential modeling capabilities. For more recent models like BASM [25] and RCL, ReST still achieves modest but consistent improvements, showing AUC gains of 0.11% over BASM and 0.42% over RCL, which demonstrates its plug-and-play flexibility across different architectures. The varying degrees of improvement across different models highlight ReST's adaptive nature in addressing the unique challenges of local lifestyle recommendations, particularly in scenarios where spatial constraints and long-tail sparsity issues are prominent.

5.4 Ablation Study (RQ 3)

To validate the effectiveness of different components in ReST, we conduct ablation studies by implementing four variants:

- ReST-1: To verify the effectiveness of hard negative sampling, we replace it with random negative sampling within each batch.
- ReST-2: To investigate the necessity of brand features in positive sample selection, we only use category loss.

Table 5: Overall performance improvement by applying ReST to various recommendation learning methods.

Method	AUC	MRR	NDCG@5	NDCG@10
DIN	0.6946	0.3977	0.3911	0.4595
DIN+ReST	0.7059	0.4061	0.4089	0.4778
Gain	+1.62%	+2.12%	+4.55%	+3.98%
TRISAN	0.7039	0.3968	0.3978	0.4633
TRISAN+ReST	0.7454	0.4426	0.4478	0.5125
Gain	+5.90%	+11.54%	+12.57%	+10.62%
BASM	0.7193	0.4168	0.4187	0.4796
BASM+ReST	0.7201	0.4227	0.4204	0.4852
Gain	+0.11%	+1.41%	+0.41%	+1.17%
RCL	0.7078	0.4327	0.4332	0.4891
RCL+ReST	0.7108	0.4322	0.4327	0.4888
Gain	+0.42%	-0.12%	-0.12%	-0.06%

- **ReST-3:** To explore the importance of category features in positive sample selection, we only use brand loss.
- **ReST-4**: To examine the necessity of item-side information for representation enhancement, we remove the warm-up network.

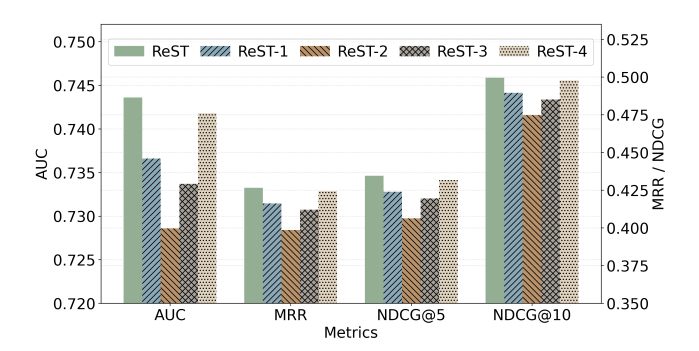


Figure 3: Ablation study on ReST.

As shown in Figure 3, all variants show performance degradation compare to the complete ReST model, demonstrating the effectiveness of each component. Specifically, ReST-1 experiences a notable decline in AUC by 0.70%, indicating that hard negative sampling is crucial for learning discriminative representations. ReST-2 and ReST-3 show more significant performance drops, with AUC decreasing by 1.49% and 1.99% respectively, which validates that both brand and category features are essential for effective positive sample selection. ReST-4 shows the smallest performance drop (0.17% in AUC), suggesting that while the warm-up network contributes to the model's performance, the core representation enhancement mechanisms remain effective even without it.

5.5 Hyper-Parameter Study (RQ 4)

In this section, we investigate the impact of various hyperparameters on model performance through extensive experiments. Specifically, we conduct experiments on: (1) different combinations of distance thresholds for positive and negative samples, (2) the number of hard negative samples k, (3) the number of clustering centers c in k-means clustering, and (4) the contrastive learning loss weight λ . The experimental results and analyses are presented as follows.

Table 6: Performance comparison with different distance thresholds (km). "∞" denotes no distance constraints are applied for contrastive samples.

Pos	Neg	AUC	MRR	NDCG@5	NDCG@10
5	5	0.7329	0.4052	0.4132	0.4810
5	10	0.7337	0.4082	0.4146	0.4826
5	30	0.7275	0.3976	0.4035	0.4738
10	5	0.7340	0.4094	0.4168	0.4842
10	10	0.7337	0.4089	0.4161	0.4836
10	30	0.7308	0.4040	0.4109	0.4792
30	5	0.7270	0.4054	0.4114	0.4777
30	10	0.7436	0.4266	0.4345	0.4996
30	30	0.7343	0.4137	0.4204	0.4869
∞	∞	0.6811	0.3310	0.3260	0.4077

Positive and negative sample distance thresholds. As shown in Table 6, we evaluate various combinations of distance thresholds for positive and negative samples. The best results are obtained with a positive threshold of 30 km and a negative threshold of 10 km, achieving an AUC of 0.7436 and NDCG@5 of 0.4345. This can be explained by two factors: (1) a larger positive threshold (30 km) captures more diverse positive interactions within a reasonable geographic range, enhancing the model's understanding of user preferences while preserving relevance; and (2) a moderate negative threshold (10 km) balances local and distant negatives, avoiding the limitations of a small threshold (5 km) and the noise of a large threshold (30 km). Without distance constraints, performance drops markedly (AUC = 0.6811), confirming that geographic proximity is critical in user–item interactions and highlighting the importance of incorporating such information in the sampling strategy.

The number of hard negative samples. As shown in Figure 4 (left), we examine the impact of the number of hard negative samples (k) on model performance. Through extensive experiments with different k values ranging from 3 to 15, we observe significant variations in model performance. The experimental results demonstrate that setting k to 9 achieves the optimal performance across all metrics, with an MRR of 0.4266 and NDCG@10 of 0.4996. This superior performance can be attributed to the balanced selection of hard negative samples. When k is set to smaller values such as 3 or 6, the model fails to capture sufficient challenging cases, resulting in suboptimal performance with AUC values of 0.7335 and 0.7354, respectively. The limited number of hard negative samples restricts the model's ability to learn discriminative features effectively. Conversely, increasing k beyond 9 leads to performance degradation. With k values of 12 and 15, the AUC drops to 0.7305 and 0.7334 respectively. This deterioration occurs because excessively hard negative samples introduce noise into the training process and potentially cause over-emphasis on challenging cases. The increased number of hard negative samples disrupts the learning balance, preventing the model from capturing the general patterns in user-item interactions.

The number of clustering centers. As shown in Figure 4 (middle), we investigate the impact of the number of clustering centers (c) in k-means clustering on model performance. We conduct comprehensive experiments with c varying from 5 to 100 to understand

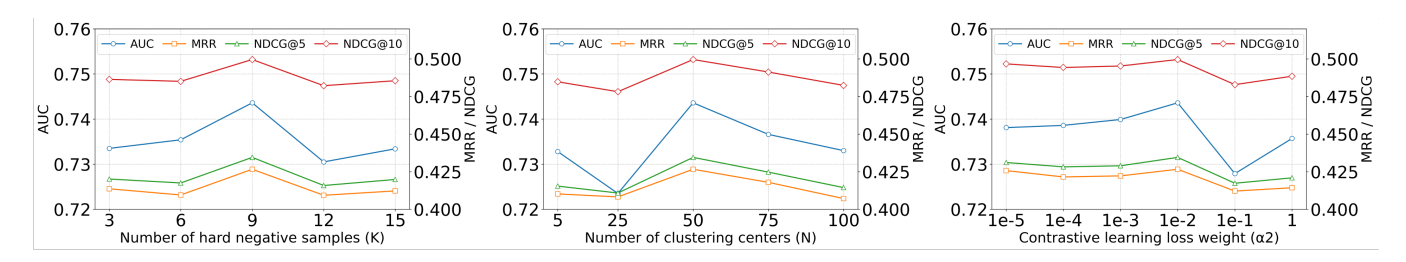


Figure 4: Performance comparison with different numbers of hard negative samples.

its influence on the model's effectiveness. The experimental results reveal distinct performance patterns across different numbers of clustering centers. With a small number of centers (c=5), the model achieves moderate performance but fails to capture fine-grained user-item interaction patterns. This insufficient granularity in clustering leads to oversimplified user behavior representations. Further reducing c to 25 results in even lower performance, with AUC decreasing to 0.7235, indicating that too few clusters cannot effectively capture the diversity of user preferences. As the number of clustering centers increases to 75 and beyond, we observe a declining trend in model performance. The AUC drops from 0.7366 with 75 centers to 0.7330 with 100 centers. This performance degradation stems from the over-fragmentation of item semantics caused by excessive clustering centers. Such fine-grained partitioning introduces noise into the representation learning process and leads the model to capture spurious distinctions between items, rather than preserving their essential characteristics for effective recommendation.

Contrastive loss weight. As shown in Figure 4 (right), we examine the influence of the contrastive learning loss weight α_2 in Eq. (13) on model performance. We conduct extensive experiments with α_2 ranging from 1e-5 to 1 to understand its impact on the model's effectiveness. The experimental results demonstrate a clear pattern of performance variation with different contrastive learning weights. With α_2 =1e-5, the model achieves an AUC of 0.7381, indicating that minimal contribution from contrastive learning is insufficient to fully leverage the benefits of contrast-aware learning. As α_2 increases to 1e-4 and 1e-3, we observe a steady improvement in performance, with AUC reaching 0.7386 and 0.7399 respectively, suggesting that stronger contrastive signals enhance the model's ability to learn discriminative features. However, when α_2 =1e-1, the performance deteriorates significantly with AUC dropping to 0.7279. This degradation continues with α_2 =1, though with a slight recovery to 0.7357. This result suggests that overly strong contrastive signals may disrupt the balance with the main task, causing the model to focus more on sample separation than task-relevant features.

5.6 Online A/B Test (RQ 5)

We conducted comprehensive online A/B testing on Kuaishou's local lifestyle short-video platform from March 14 to March 26, 2025, serving millions of daily active users. The platform faces unique challenges in content distribution, particularly with long-tail effects where high-quality but less popular content struggles to gain adequate exposure. Therefore, we integrate the ReST framework into ranking baseline model, aiming to enhance the quality of ID representations, improve the distribution efficiency of mid- and

Table 7: Online performance comparison

Metrics		ade	Experience		
Metrics	GMV	Orders	Play Time	Clicks	
Ours vs Base	+2.804%	+1.285%	+4.188%	+1.226%	

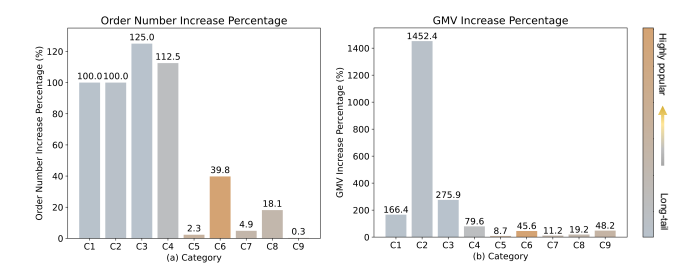


Figure 5: Performance improvement in orders and GMV across item popularity: long-tail items show greater relative gains due to naturally lower baseline GMV.

small-scale items, and ultimately boost overall GMV and order numbers in Kuaishou's local lifestyle platform.

Overall Performance. The results of our online A/B testing are presented in Table 7, where we evaluate both transaction-related and user-experience metrics. On the transaction side, our method improves GMV by 2.804% and increases Orders by 1.285%. For user experience, play Time rises by 4.188% and clicks by 1.226%. These gains are significant in the context of local-lifestyle recommendations, where spatial constraints and item diversity make improvements challenging. The 4.188% lift in play Time indicates stronger content relevance and user engagement, while the 2.804% GMV uplift demonstrates effective conversion stimulation across Kuaishou, driving overall business growth.

Long-tail Performance. Figure 5 demonstrates the effectiveness of our method in enhancing both order numbers and GMV across different categories. Specifically, our method not only boosts the performance of highly popular items, with order number increases ranging from 0.3% to 39.8% and GMV increases from 8.7% to 48.2%, but also significantly improves the sales of long-tail items. For long-tail items, the order number increase ranges from 100.0% to 125.0%, and the GMV increase ranges from 79.6% to 1452.4%. This balanced approach ensures that even less popular categories benefit from the overall strategy, leading to a more comprehensive and effective sales improvement.

6 Conclusions

To address the challenges of spatial constraints and the long-tail effect in local-life recommendation, we propose ReST, a plug-andplay ID representation enhancement framework designed to tackle spatially-constrained scenarios.ReST introduces a novel ID representation enhancement strategy using self-supervised learning, tailored to the unique characteristics of local lifestyle services, effectively replacing traditional methods that often underperform in these scenarios. Extensive experiments demonstrate that our method outperforms state-of-the-art spatiotemporal and long-tail modeling approaches, with each proposed module contributing to improved overall performance. Furthermore, comprehensive evaluations on cold-start datasets confirm ReST's ability to significantly enhance long-tail item representation and improve robustness under sparse interaction conditions. Online A/B testing also validates the effectiveness of our framework in real-world industrial deployment, showing notable improvements in both GMV and order volume, as well as better prediction of long-tail items. Importantly, the plug-and-play nature of ReST allows seamless integration with various backbone recommendation models, consistently boosting performance across different systems.

References

- A. v. d. Oord, Y. Li, and O. Vinyals, "Representation learning with contrastive predictive coding," arXiv preprint arXiv:1807.03748, 2018.
 C. Wu, F. Wu, T. Qi, and Y. Huang, "User modeling with click preference and
- [2] C. Wu, F. Wu, T. Qi, and Y. Huang, "User modeling with click preference and reading satisfaction for news recommendation," in Proceedings of the Twenty-Ninth International Joint Conference on Artificial Intelligence, ser. IJCAI'20, 2021.
- [3] P. Mai, H. Jiang, R. Yan, Y. Yang, Z. Huang, and Y. Pang, "Knowledge graph unlearning to defend language model against jailbreak attack," in *The Second Tiny Papers Track at ICLR 2024*, 2024. [Online]. Available: https://openreview.net/forum?id=gqTUlesy4H
- [4] S. Zhao, W. Chen, B. Shi, L. Zhou, S. Lin, and H. Wan, "Spatial-temporal knowledge distillation for takeaway recommendation," in *Proceedings of the AAAI Conference* on Artificial Intelligence, vol. 39, no. 12, 2025, pp. 13365–13373.
- [5] S. Lin, Y. Yu, X. Ji, T. Zhou, H. He, Z. Sang, J. Jia, G. Cao, and N. Hu, "Spatiotemporal-enhanced network for click-through rate prediction in locationbased services," arXiv preprint arXiv:2209.09427, 2022.
- [6] S. Luo, C. Ma, Y. Xiao, and L. Song, "Improving long-tail item recommendation with graph augmentation," in Proceedings of the 32nd ACM international conference on information and knowledge management, 2023, pp. 1707–1716.
- [7] X. Xie, J. Niu, L. Deng, D. Wang, J. Zhang, Z. Wu, K. Bian, G. Cao, and B. Cui, "Hierarchical interest modeling of long-tailed users for click-through rate prediction," in 2023 IEEE 39th International Conference on Data Engineering (ICDE). IEEE, 2023, pp. 3058–3071.
- [8] Y. Zhang, R. Wang, D. Z. Cheng, T. Yao, X. Yi, L. Hong, J. Caverlee, and E. H. Chi, "Empowering long-tail item recommendation through cross decoupling network (cdn)," in Proceedings of the 29th ACM SIGKDD Conference on Knowledge Discovery and Data Mining, 2023, pp. 5608–5617.
- [9] Z. Zhao, K. Zhou, X. Wang, W. X. Zhao, F. Pan, Z. Cao, and J.-R. Wen, "Alleviating the long-tail problem in conversational recommender systems," in *Proceedings of* the 17th ACM Conference on Recommender Systems, 2023, pp. 374–385.
- [10] B. Hidasi, A. Karatzoglou, L. Baltrunas, and D. Tikk, "Session-based recommendations with recurrent neural networks," arXiv preprint arXiv:1511.06939, 2015.
- [11] Y. Zhang, Y. Liu, Y. Xu, H. Xiong, C. Lei, W. He, L. Cui, and C. Miao, "Enhancing sequential recommendation with graph contrastive learning," arXiv preprint arXiv:2205.14837, 2022.
- W. Chen, H. Wan, S. Guo, H. Huang, S. Zheng, J. Li, S. Lin, and Y. Lin, "Building and exploiting spatial-temporal knowledge graph for next poi recommendation," *Knowledge-Based Systems*, vol. 258, p. 109951, 2022.
 Y. Shin, J. Choi, H. Wi, and N. Park, "An attentive inductive bias for sequential
- [13] Y. Shin, J. Choi, H. Wi, and N. Park, "An attentive inductive bias for sequential recommendation beyond the self-attention," in *Proceedings of the AAAI Conference* on Artificial Intelligence, vol. 38, no. 8, 2024, pp. 8984–8992.
- [14] S. Kang, W. Kweon, D. Lee, J. Lian, X. Xie, and H. Yu, "Distillation from heterogeneous models for top-k recommendation," in *Proceedings of the ACM Web Conference* 2023, 2023, pp. 801–811.
- [15] B. Du, S. Lin, J. Gao, X. Ji, M. Wang, T. Zhou, H. He, J. Jia, and N. Hu, "Basm: A bottom-up adaptive spatiotemporal model for online food ordering service," in 2023 IEEE 39th International Conference on Data Engineering (ICDE). IEEE, 2023,

- pp. 3549-3562.
- [16] M. Volkovs, G. Yu, and T. Poutanen, "Dropoutnet: Addressing cold start in recommender systems," Advances in neural information processing systems, vol. 30, 2017
- [17] X. Xie, F. Sun, Z. Liu, S. Wu, J. Gao, J. Zhang, B. Ding, and B. Cui, "Contrastive learning for sequential recommendation," in 2022 IEEE 38th international conference on data engineering (ICDE). IEEE, 2022, pp. 1259–1273.
- [18] J. B. Schafer, J. A. Konstan, and J. Riedl, "E-commerce recommendation applications," Data mining and knowledge discovery, vol. 5, pp. 115–153, 2001.
- [19] O. Celma, "Music recommendation," in Music recommendation and discovery: The long tail, long fail, and long play in the digital music space. Springer, 2010, pp. 43–85.
- [20] J. Hu, L. Shen, S. Albanie, G. Sun, and E. Wu, "Squeeze-and-excitation networks," 2019. [Online]. Available: https://arxiv.org/abs/1709.01507
- [21] Q. Cui, C. Zhang, Y. Zhang, J. Wang, and M. Cai, "St-pil: Spatial-temporal periodic interest learning for next point-of-interest recommendation," in Proceedings of the 30th ACM International conference on information & knowledge management, 2021, pp. 2960–2964.
- [22] Y. Qi, K. Hu, B. Zhang, J. Cheng, and J. Lei, "Trilateral spatiotemporal attention network for user behavior modeling in location-based search," in *Proceedings of the 30th ACM International Conference on Information & Knowledge Management*, 2021, pp. 3373–3377.
- [23] H. Chi, H. Xu, M. Liu, Y. Bei, S. Zhou, D. Liu, and M. Zhang, "Modeling spatiotemporal periodicity and collaborative signal for local-life service recommendation," arXiv preprint arXiv:2309.12565, 2023.
- [24] S. Lin, J. Pei, T. Zhou, H. He, J. Jia, and N. Hu, "Exploring the spatiotemporal features of online food recommendation service," in Proceedings of the 46th International ACM SIGIR Conference on Research and Development in Information Retrieval, 2023, pp. 3354–3358.
- [25] B. Du, S. Lin, J. Gao, X. Ji, M. Wang, T. Zhou, H. He, J. Jia, and N. Hu, "Basm: A bottom-up adaptive spatiotemporal model for online food ordering service," in 2023 IEEE 39th International Conference on Data Engineering (ICDE). IEEE, 2023, pp. 3549–3562.
- [26] C. Duan, W. Fan, W. Zhou, H. Liu, and J. Wen, "Clsprec: Contrastive learning of long and short-term preferences for next poi recommendation," in Proceedings of the 32nd ACM international conference on information and knowledge management, 2023, pp. 473–482.
- [27] S. Li, W. Chen, B. Wang, C. Huang, Y. Yu, and J. Dong, "Mcn4rec: Multi-level collaborative neural network for next location recommendation," ACM Transactions on Information Systems, vol. 42, no. 4, pp. 1–26, 2024.
- [28] J. Li and G. Zhang, "Fragment and integrate network (fin): A novel spatial-temporal modeling based on long sequential behavior for online food ordering click-through rate prediction," in Proceedings of the 32nd ACM International Conference on Information and Knowledge Management, 2023, pp. 4688–4694.
- [29] M. Volkovs, G. Yu, and T. Poutanen, "Dropoutnet: Addressing cold start in recommender systems," Advances in neural information processing systems, vol. 30, 2017.
- [30] F. Pan, S. Li, X. Ao, P. Tang, and Q. He, "Warm up cold-start advertisements: Improving ctr predictions via learning to learn id embeddings," in Proceedings of the 42nd International ACM SIGIR Conference on Research and Development in Information Retrieval, 2019, pp. 695–704.
- [31] Y. Ge, S. Liu, R. Gao, Y. Xian, Y. Li, X. Zhao, C. Pei, F. Sun, J. Ge, W. Ou et al., "Towards long-term fairness in recommendation," in Proceedings of the 14th ACM international conference on web search and data mining, 2021, pp. 445–453.
- [32] X. Xie, F. Sun, Z. Liu, S. Wu, J. Gao, J. Zhang, B. Ding, and B. Cui, "Contrastive learning for sequential recommendation," in 2022 IEEE 38th international conference on data engineering (ICDE). IEEE, 2022, pp. 1259–1273.
- [33] Z. Zhao, K. Zhou, X. Wang, W. X. Zhao, F. Pan, Z. Cao, and J.-R. Wen, "Alleviating the long-tail problem in conversational recommender systems," in *Proceedings of* the 17th ACM Conference on Recommender Systems, 2023, pp. 374–385.
- [34] X. Xie, J. Niu, L. Deng, D. Wang, J. Zhang, Z. Wu, K. Bian, G. Cao, and B. Cui, "Hierarchical interest modeling of long-tailed users for click-through rate prediction," in 2023 IEEE 39th International Conference on Data Engineering (ICDE). IEEE, 2023, pp. 3058–3071.
- [35] K. Balasubramanian, A. Alshabanah, E. Markowitz, G. Ver Steeg, and M. Annavaram, "Biased user history synthesis for personalized long-tail item recommendation," in *Proceedings of the 18th ACM Conference on Recommender Systems*, 2024, pp. 189–199.
- [36] Y. Gao, P. Lin, D. Wang, F. Mei, X. Zhao, S. Xu, and J. Hu, "Ppm: A pre-trained plug-in model for click-through rate prediction," in Companion Proceedings of the ACM Web Conference 2024, 2024, pp. 311–318.
- [37] G. Lee, K. Kim, and K. Shin, "Post-training embedding enhancement for long-tail recommendation," in Proceedings of the 33rd ACM International Conference on Information and Knowledge Management, 2024, pp. 3857–3861.
- [38] S. Park, M. Yoon, M. Choi, and J. Lee, "Temporal linear item-item model for sequential recommendation," in Proceedings of the Eighteenth ACM International Conference on Web Search and Data Mining, 2025, pp. 354–362.

- [39] G. Zhou, X. Zhu, C. Song, Y. Fan, H. Zhu, X. Ma, Y. Yan, J. Jin, H. Li, and K. Gai, Deep interest network for click-through rate prediction," in Proceedings of the 24th ACM SIGKDD international conference on knowledge discovery & data mining, 2018, pp. 1059-1068.
- [40] Z. Wang, Y. Shen, Z. Zhang, L. He, Y. Li, H. Gu, and Y. Zhang, "Relative contrastive learning for sequential recommendation with similarity-based positive sample selection," in Proceedings of the 33rd ACM International Conference on Information and Knowledge Management, 2024, pp. 2493-2502.
- [41] S. Zhao, W. Chen, B. Shi, L. Zhou, S. Lin, and H. Wan, "Spatial-temporal knowledge distillation for takeaway recommendation," in Proceedings of the AAAI Conference on Artificial Intelligence, vol. 39, no. 12, 2025, pp. 13365-13373.
- [42] G. Wang, Q. Luo, W. Hu, P. Yao, W. Zeng, G. Zhou, and K. Gai, "Fim: Frequencyaware multi-view interest modeling for local-life service recommendation," arXiv preprint arXiv:2504.17814, 2025.
- [43] J. A. Hanley and B. J. McNeil, "The meaning and use of the area under a receiver operating characteristic (roc) curve." Radiology, vol. 143, no. 1, pp. 29-36, 1982.
- [44] E. M. Voorhees et al., "The trec-8 question answering track report." in Trec, vol. 99, 1999, pp. 77-82.
- [45] K. Järvelin and J. Kekäläinen, "Cumulated gain-based evaluation of ir techniques," ACM Transactions on Information Systems (TOIS), vol. 20, no. 4, pp. 422-446, 2002.
- [46] X. He, L. Liao, H. Zhang, L. Nie, X. Hu, and T.-S. Chua, "Neural collaborative filtering," in Proceedings of the 26th international conference on world wide web, 2017, pp. 173-182.
- [47] X. Luo, J. Cao, T. Sun, J. Yu, R. Huang, W. Yuan, H. Lin, Y. Zheng, S. Wang, Q. Hu et al., "Qarm: Quantitative alignment multi-modal recommendation at kuaishou,"

- arXiv preprint arXiv:2411.11739, 2024.
- [48] C. C. Robusto, "The cosine-haversine formula," The American Mathematical Monthly, vol. 64, no. 1, pp. 38-40, 1957.
- G. Wang, Q. Luo, W. Hu, P. Yao, W. Zeng, G. Zhou, and K. Gai, "Fim: Frequencyaware multi-view interest modeling for local-life service recommendation," arXiv preprint arXiv:2504.17814, 2025.
- [50] H. Chi, H. Xu, M. Liu, Y. Bei, S. Zhou, D. Liu, and M. Zhang, "Modeling spatiotemporal periodicity and collaborative signal for local-life service recommendation," arXiv preprint arXiv:2309.12565, 2023.
- [51] W. Wang, H. Yin, L. Chen, Y. Sun, S. Sadiq, and X. Zhou, "Geo-sage: A geographical sparse additive generative model for spatial item recommendation," in Proceedings of the 21th ACM SIGKDD international conference on knowledge discovery and data mining, 2015, pp. 1255-1264.
- [52] Q. Fang, C. Xu, M. S. Hossain, and G. Muhammad, "Stcaplrs: A spatial-temporal context-aware personalized location recommendation system," ACM Transactions on Intelligent systems and technology (TIST), vol. 7, no. 4, pp. 1-30, 2016.
- [53] Y. LeCun, Y. Bengio, and G. Hinton, "Deep learning," nature, vol. 521, no. 7553,
- [54] J. Liu, H. Li, Y. Gao, H. Yu, and D. Jiang, "A geohash-based index for spatial data management in distributed memory," in 2014 22Nd international conference on geoinformatics. IEEE, 2014, pp. 1–4.
 [55] D. Arthur and S. Vassilvitskii, "k-means++: The advantages of careful seeding,"
- Stanford, Tech. Rep., 2006.